Journal of Power Sources 210 (2012) 15–20

Contents lists available at SciVerse ScienceDirect

Journal of Power Sources

journal homepage: www.elsevier.com/locate/jpowsour

Application of a composite structure of carbon nanoparticles and Nb–TiO_2 nanofibers as electrocatalyst support for PEM fuel cells

Alex Bauer[a], Rob Hui[a,*], Anna Ignaszak[a], Jiujun Zhang[a], Deborah J. Jones[b]

[a] Institute for Fuel Cell Innovation, National Research Council of Canada, 4250 Wesbrook Mall, Vancouver, BC, Canada V6T 1W5
[b] Institut Charles Gerhardt, Agrégats, Interfaces et Matériaux pour l'Energie, UMR CNRS 5253, Université Montpellier II, 34095 Montpellier Cedex 5, France

ARTICLE INFO

Article history:
Received 4 January 2012
Received in revised form 22 February 2012
Accepted 23 February 2012
Available online 3 March 2012

Keywords:
Fuel cells
Conductive ceramics
Catalyst support
Nanofibers
Doped titanium oxide

ABSTRACT

Platinum catalyst nanoparticles (20 wt.%) were deposited on a mixed support, which consisted of 25 at.% Nb doped TiO_2 nanofibers and carbon agglomerates. XRD analysis revealed that titania was present in the rutile phase. The catalyst was characterized electrochemically with respect to durability and oxygen reduction activity. Based on cyclic voltammetry tests, the Nb–TiO_2/C supported catalyst was more stable compared to a commercially available carbon supported Pt catalyst (E-tek) over 1000 cycles. The apparent active Pt area decreased by 5% due to cycling, whereas in the case of Pt/C the decrease was 23%. The oxygen reduction performance was comparable for both cases. For example, during the anodic sweep the mass activity at 0.9 V vs. the reversible hydrogen electrode (RHE) was 19 A g_{Pt}^{-1} and 20 A g_{Pt}^{-1} for the freshly prepared in-house prepared and commercial catalysts, respectively. After the durability experiment both types of catalysts yielded a mass activity of 17 A g_{Pt}^{-1}. Fuel cell tests with a single cell configuration were also carried out with the Nb–TiO_2/C supported catalyst on the cathode side (gas diffusion electrode), yielding a peak power density of 0.34 W cm^{-2} at 75 °C when pure oxygen was supplied on the cathode side.

1. Introduction

Ceramic catalyst support materials were widely researched in recent years due to their promising characteristics for applications in proton exchange membrane (PEM) fuel cells, in particular high temperature (HT) PEM fuel cells, where high catalyst durability is required [1–10]. The feasibility of such ceramic catalyst supports in HT PEM fuel cells operated in the temperature range of 120–180 °C can be rationalized by the conductivity increase of the ceramic support with increasing temperature. As recognized, the benefits of operating at higher temperatures include high tolerance toward contaminants, improved reaction kinetics, simplified water management, and fast heat dispersion reducing the load of the cooling system. Unfortunately, the corrosion or oxidation of practical Pt-based catalysts is inevitable at high temperature and high electrode potential. Therefore, ceramic materials represent a viable alternative as catalyst supports due to their well known corrosion resistance. Among those ceramic materials, titanium dioxide based supports were identified as being particularly stable [2,7,11].

In general, the conductivity of titania is rather low. Therefore the support is typically doped with metals that have an atomic radius similar to Ti, such as Nb or Ta, which yields a certain fraction of Ti^{3+} species. The conductivity can also be increased by exposing the TiO_2 to reducing conditions at high temperatures (~650 to 850 °C) in order to form substoichiometric titanium oxides, such as Ti_4O_7 [12–16]. Huang et al. [17,18] demonstrated the feasibility of a 25 at.% Nb doped TiO_2 support, which was treated at high temperature under reducing conditions. The fuel cell performance obtained with this support was comparable to the output recorded when operating with carbon supported Pt catalyst (Pt/C).

Another approach toward improving the conductivity of such metal oxide support structures is to incorporate a certain amount of carbon so that a composite is formed, and then used as the catalyst support (TiO_2–C) [19–24]. It was demonstrated previously for the case of mesoporous carbon supports that TiO_2 stabilized carbon is more durable than carbon alone while yielding similar oxygen reduction activity [23]. Comparable fuel cell performance with TiO_2–C supported Pt relative to Pt supported on carbon was reported [24].

In order to improve the surface area and catalyst distribution, TiO_2 supports can be designed having a variety of morphologies, such as nanoparticles, mesoporous spheres, and nanofibers [1,7,11,25,26].

In this work, we report the synthesis and application of a TiO_2-based support, which consists of Nb doped TiO_2 nanofibers interlinked with carbon agglomerates. The nanofibers were

* Corresponding author. Tel.: +1 604 221 3111; fax: +1 604 221 3001.
E-mail address: rob.hui@nrc-cnrc.gc.ca (R. Hui).

0378-7753/$ – see front matter.
doi:10.1016/j.jpowsour.2012.02.093

produced by electrospinning, which is a technique that generally allows good control of the fiber diameter [10,24]. In our previous work, the electrospun fibers were treated by air calcination at 500 °C for 3 h, which led to a pure Nb-doped TiO_2 support with no carbon component [11]. In this work, we intentionally maintain some residue of carbon agglomerates on the nanofibers to improve the support's conductivity. This support was then catalyzed with Pt nanoparticles using a straightforward microwave assisted deposition technique with ethylene glycol acting as both a solvent and a template. The electrochemical performance of this in-house prepared catalyst material was evaluated in terms of both catalyst activity and stability toward the oxygen reduction reaction, and the obtained results were compared to the performance of a commercially available carbon supported catalyst. Fuel cell experiments were also conducted with a single cell setup with an active membrane electrode assembly (MEA) area of 5 cm^2.

2. Experimental

2.1. Catalyst support synthesis

For the Nb-doped TiO_2 solution preparation, a precursor solution with 1.5 g of titanium(IV)isopropoxide (98%, Acros), 3 ml of acetic acid (Fisher) and 3 ml of anhydrous ethanol as well as 434 μl niobium ethoxide (corresponding to 25 at.% Nb) was mixed and then sonicated for 20 min. For the carbon source solution, 0.3 g polyvinyl pyrrolidone (Alfa Aesar) was dissolved in 7.5 ml anhydrous ethanol (Commercial Alcohols Inc.) via sonication at $T = 80$ °C for 1 h. After that, both solutions were combined and sonicated for 20 min, and then filled into a syringe, which had a stainless steel needle with an inner diameter of 0.5 mm for electrospinning, which was performed at ambient conditions [11]. During the electrospinning process the feed rate was 0.7 ml h^{-1}, and the distance between the tip of the needle and the collector plate was 6 cm. A constant voltage of 11.55 kV was applied.

After the electrospinning procedure was completed, the fibers were maintained at ambient conditions for 6 h to complete the inorganic polymer hydrolysis and condensation. The material was then treated in a hydrogen gas stream. First, the temperature was ramped to 500 °C at a rate of 3 °C min^{-1}. The temperature was kept constant at 500 °C for 2 h, and then the temperature was increased at the same rate to 850 °C and then held constant for 6 h. The temperature was then lowered to 20 °C at a rate of 3 °C min^{-1}. This way, a composite support (Nb–TiO_2–C) was expected to be obtained. Pt supported on carbon (20 wt.% Pt on Vulcan) was supplied as commercial available products from E-Tek.

2.2. Pt nanoparticle deposition

The Pt nanoparticle catalyst was dispersed onto the Nb–TiO_2–C nanofiber support by an intermittent microwave heating polyol method [27–29]. In this process, Nb–TiO_2–C (50 mg) was mixed with 20 ml ethylene and 29 mg H_2PtCl_6 (Aldrich), which corresponded to a Pt loading of 20 wt.% The slurry was then stirred vigorously for 20 min. The pH of the bath was adjusted to a value of 8 by gradually introducing a 1 M NaOH in ethylene glycol solution with a micropipette. The following duty cycle was carried out four times: (i) heating of the bath for 1 min in a microwave oven at a setting of 600 W and (ii) briefly stirring the mixture and letting it cool at ambient conditions for 5 min. Once these heating-cooling intervals were completed, centrifugation at 10,000 rpm (Sorvall Legend RT+, Thermo Scientific) was performed for 20 min. Then the solvent was replaced with fresh deionized water. The centrifuging and solvent replacement procedure was carried out three more times, and then the sample was finally dried in an oven at 80 °C overnight to form supported Pt catalyst (Pt/Nb–TiO_2–C).

2.3. XRD, EDX and TEM analysis

The XRD pattern for the uncatalyzed support was recorded with a Bruker D8 diffractometer equipped with a graphite monochromator and a vertical goniometer, utilizing Cu Kα radiation. The 2θ regime was scanned at a rate of 6° min^{-1} with a step size of 0.02° from 15° to 90°.

The elemental analysis was performed using an EDX analyzer (Oxford Instruments, UK) with a resolution of 60 eV and a spot diameter of 5 nm, coupled with a Hitachi S-3500N scanning electron microscope. The microscope was operated at a voltage of 20 kV, an emission current of 90 μA, and 70 to 100-fold magnification. The amount of elements was quantified using the Isis Series 300 software, Version 3.2.

Transmission electron micrographs were obtained with a Hitachi H7600 microscope, which was operated at 100 kV in bright field mode. This work was carried out at the BioImaging facilities at the University of British Columbia.

2.4. Electrode preparation and electrochemical testing

For the working electrode preparation, the catalyst powder was dispersed on a glassy carbon rotating disk electrode (RDE) (Pine Instrument) with a geometric area of 0.20 cm^2. The catalyst powder was mixed with isopropanol and dispersed by sonication for 20 min. The ink was applied to the RDE surface with a micropipette so that a Pt loading of 48 μg cm^{-2} was present. A Pt wire counter electrode and a $Hg/HgSO_4$ reference electrode, which contained a 30 wt.% sulfuric acid solution (Koslow Scientific), were employed. A Nafion® film was cast by applying 7.1 μl of a 0.05 wt.% Nafion® in methanol solution onto the dry powder coated RDE to prevent detachment of the catalyst. The coated electrode was cycled 20 times in N_2 purged 0.5 M H_2SO_4 between 0.05 V and 1.2 V vs. RHE (reversible hydrogen electrode) at a scan rate of 50 mV s^{-1}.

The electrochemical experiments were carried out using a Solartron multipotentiostat instrument (controlled by Corrware software, Scribner Associates Inc., USA). The electrochemical catalyst stability was monitored over 1000 cycles in the same potential range between 0.05 V and 1.2 V vs. RHE at 100 mV s^{-1}. The active Pt surface was estimated based on the H_2 desorption charge, which was measured during the anodic sweeps between 0.05 V and 0.35 V vs. RHE. The hydrogen desorption charge measured during the 100th cycle was used to quantify the active area for the fresh catalyst state. For Pt surface calculation, a standard hydrogen desorption charge of 210 μC cm^{-2} on a pure Pt surface is assumed [30].

Oxygen reduction reaction (ORR) tests were conducted by cyclic voltammetry in an O_2-saturated 0.5 M H_2SO_4 aqueous electrolyte. The potential was decreased from 1.1 V to 0.2 V vs. RHE and then ramped back to the initial setting at a scan rate of 5 mV s^{-1}. During this voltage scan, the electrode rotation rate was maintained at1600 rpm. The ORR activity was determined for fresh catalysts and catalysts that were subjected to 1000 voltammetric cycles as described above. All electrochemical tests were carried out at 20 °C and ambient pressure. All current density values are reported as current per geometric electrode area.

2.5. Membrane electrode assembly fabrication and fuel cell experiments

For fabrication of fuel cell membrane electrode assembly (MEA), the gas diffusion layer (GDL) used in this study is 35DC from SGL group with 20 wt.% PTFE loading. The half-MEA consists of NR-212

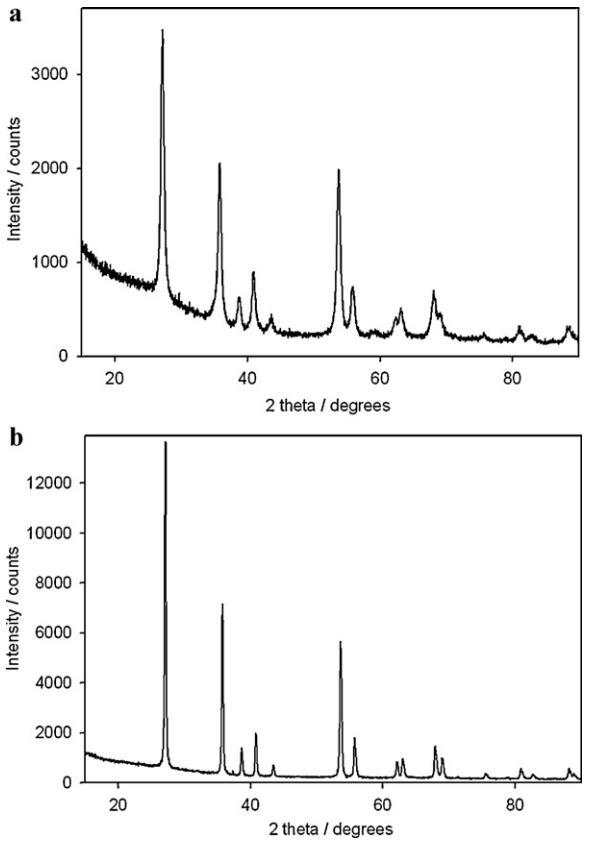

Fig. 1. XRD patterns for Nb doped titania as contained in a support structure that also contains carbon (a) and without carbon (b). Both graphs show the characteristic peaks for the rutile phase.

membrane and single side coated catalyst of 0.4 mg Pt cm^{-2} from Ion-Power. The cathode was prepared by brushing an ink, which consisted of isopropanol, Pt/Nb–TiO_2–C, and Nafion® (~25 wt.% per dry mass), onto a gas diffusion layer, which was placed on a hot plate (T = 80 °C) to facilitate solvent evaporation. After drying, an additional Nafion® layer having a loading of 0.2 mg cm^{-2} was brushed on. The cathode and the anode catalyst coated membrane as well as the anode gas diffusion layer were stacked together using a hot press (conditions: 140 °C, ~450 kg, 5 min) to form a MEA. The anode and cathode Pt loadings were 0.3 mg cm^{-2} and 0.4 mg cm^{-2}, respectively. The active geometric MEA area was 5 cm^2. The membrane electrode assembly was conditioned in situ in galvanostatic mode by adjusting the current density so that the voltage would alternate between ~0.7 V (3 min) and ~0.4 V (5 min) until the voltage stabilized. This state was achieved after ~2 h. The cell testing temperature was 75 °C and the relative humidity was 100% without pressurization. The hydrogen and oxidant (air or O_2) flow rates were 0.5 l min^{-1} and 1 l min^{-1}, respectively.

3. Results and discussion

3.1. XRD analysis

Fig. 1(a) shows the XRD pattern for the Nb–TiO_2 support synthesized and treated as described in Section 2.1. It is evident from the peak positions in the diffractogram that the rutile structure was formed [25]. Other groups also reported the formation of the rutile phase under similar heat treatment conditions [7,18]. Fig. 1(b) shows the diffractogram for a sample that was air-calcined at 500 °C for 3 h before treatment in H_2 (ramp to 500 °C, dwell for 2 h, ramp to 850 °C, dwell for 6 h). The peak positions were identical to those

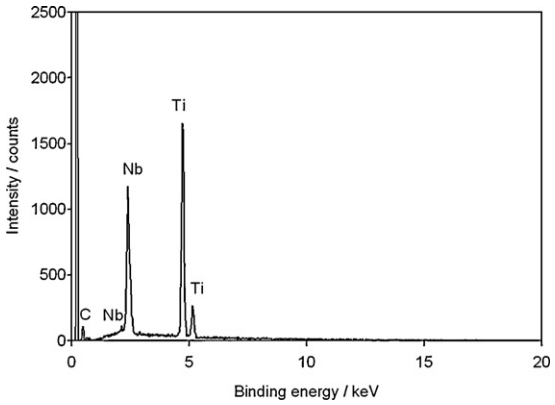

Fig. 2. Sample EDX spectrum for the Nb doped titania and carbon mixed compound support.

shown in Fig. 1(a), but the intensities are significantly higher. It is hypothesized that the presence of carbon in the sample, which was not air-calcined, decreases the peak intensity.

3.2. EDX analysis

The atomic ratio of Ti:Nb and the amount of carbon present in the support material was quantified by EDX. The Ti:Nb ratio was 2.9:1, which is close to the targeted ratio of 3:1. The metal to carbon weight ratio varied considerably from 5:1 to 1:4 depending on the point of measurement. Therefore it can be concluded that the amount of carbon is not evenly distributed relative to the titania fibers. Fig. 2 shows a typical EDX spectrum obtained for the TiO_2 fiber/carbon mixture.

3.3. TEM imaging

The micrographs shown in Fig. 3 indicate that the catalyst was dispersed homogeneously on the titania fiber surfaces with a diameter Pt of ~5 to 10 nm. Agglomerates of ~20 to 30 nm in diameter were also observed. The fiber diameter varied from 80 nm to 100 nm, and the length of the fibers ranged from ~0.5 μm to ~2 μm. The dark regions shown in the micrographs indicate carbon agglomerates (diameter = ~25 to 50 nm), which were also coated with Pt catalyst nanoparticles. The distribution of carbon relative to the Nb doped TiO_2 fibers is inhomogeneous, which is consistent with the observations by EDX. It was thus confirmed that some regions are relatively carbon-rich in comparison to others. In general, there was good connectivity between titania and carbon, which is crucial for the enhanced electronic conductivity relative to the metal oxide without carbon, since the contact resistance between the titania fibers can be very detrimental.

3.4. Voltammetric tests

The cyclic voltammetry durability tests conducted with Pt deposited on the Nb–TiO_2–C composite and carbon are shown in Fig. 4(a) and (b), respectively. The measured electrochemical active surface area (ECSA) for Pt/Nb–TiO_2–C and Pt/C after 100 cycles is 1.3–5.0 m^2 g^{-1} and 17.1 m^2 g^{-1}, respectively. With the ceramic–carbon based support the loss in the active Pt surface area was 4% and 5% after 500 and 1000 cycles, respectively. By contrast, with Pt supported on carbon, the active area decreased by 10% after 500 cycles and by 23% after 1000 cycles compared to the state of the electrode after 100 cycles. One reason for the higher stability of the composite support could be that Pt was deposited predominantly on the Nb doped TiO_2 fibrous structure. Fig. 5 shows the

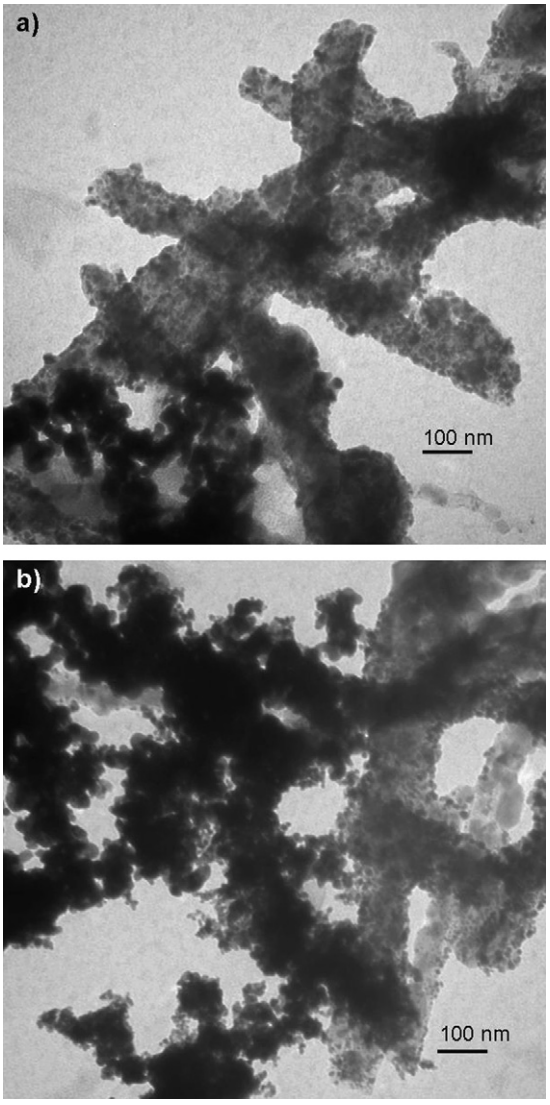

Fig. 3. TEM micrographs of Pt dispersed on the mixed Nb doped TiO_2 nanofiber–carbon substrate. The micrographs show examples of regimes with relatively low (a) and higher (b) carbon content, respectively.

correlation between progressive cycling and the remaining active Pt area as estimated from the hydrogen desorption charge.

Oxygen reduction experiments were carried out conducting full cycles for each catalyst. Fig. 6 shows the 5th sweep for each composition. During the cathodic sweep the mass activity observed for the fresh E-Tek catalyst was 10 A g_{Pt}^{-1}, whereas Pt supported on Nb doped titania–carbon composite yielded 15 A g_{Pt}^{-1}. On the reverse scan the commercial catalyst marginally outperformed the in-house prepared materials; i.e., 20 A g_{Pt}^{-1} vs. 19 A g_{Pt}^{-1} in terms of mass activity. When the ORR activity was measured after the durability test both catalysts yielded 17 A g_{Pt}^{-1} during the anodic sweep. On the cathodic scan with the 'aged' catalysts the E-tek catalyst yielded 4 A g_{Pt}^{-1} while a mass activity of 9 A g_{Pt}^{-1} was obtained with the titania based support.

Therefore in the kinetic regime the overall performance of Pt/Nb–TiO_2–C was comparable to Pt/C or higher depending on the point of reference. The di/dE slope is steeper for the commercially available catalyst, as shown in the potential regime between 0.95 V and 0.8 V vs. RHE, which can be explained by the higher conductivity of the carbon support. The conductivity of Vulcan XC-72 carbon (E-Tek catalyst) is 3 S cm^{-1} [31], whereas a value of 0.1 S cm^{-1} was obtained for the in-house

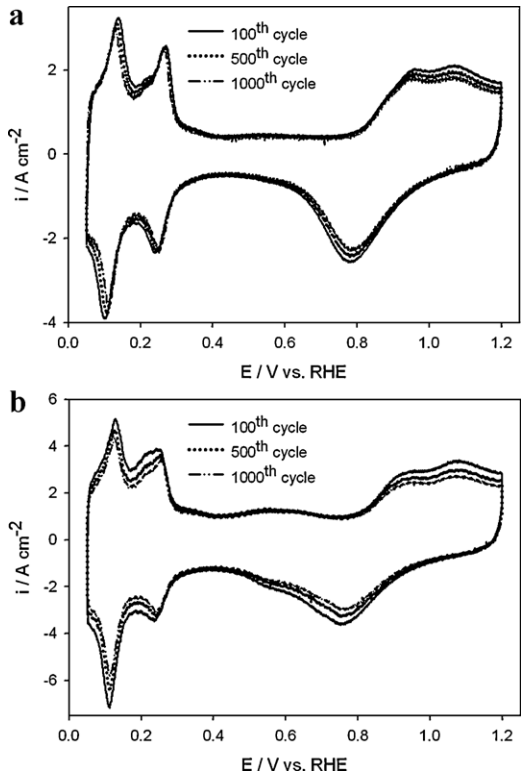

Fig. 4. Voltammetric stability experiment conducted with Pt supported on the Nb–TiO_2 nanofiber–carbon composite (a) and Pt supported on commercially available carbon (E-Tek) (b). Conditions: 0.5 M H_2SO_4 (N_2 purged), potential scan rate = 100 mV s^{-1}.

prepared composite support. The conductivity of the in-house prepared support was measured using a resistance meter and a hollow Teflon cylinder containing the uncatalyzed powder compressed between two copper coated brass pistons, which functioned as the conductivity probes. This measurement was corroborated by an impedance test using the same cylinder–probe setup.

The mass transport limited current density was higher for the commercial catalyst due to the higher specific Pt surface area. It should be noted that with a Nb–TiO_2–C support that was air calcined before H_2 treatment the mass activity was ~4 times lower compared to the support that was treated in hydrogen exclusively (results not shown). The absence of carbon in this case resulted in a lower support conductivity, which led to a decrease of the ORR performance.

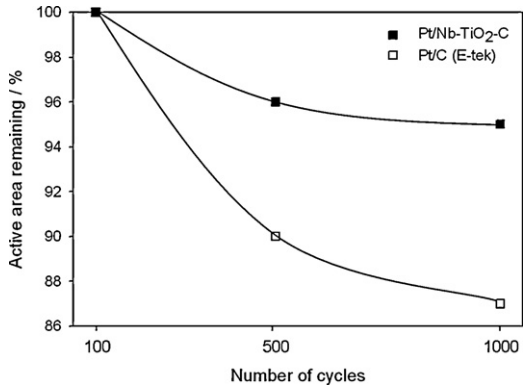

Fig. 5. Active Pt area remaining relative to the state after 100 cycles. Platinum supported on Nb–TiO_2–carbon composite compared with commercially available Pt supported on Vulcan XC-72 carbon.

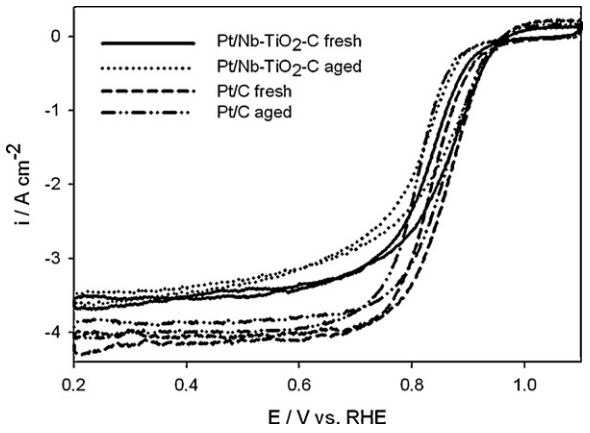

Fig. 6. Oxygen reduction linear sweep voltammetry experiments conducted with Pt supported on Nb–TiO_2–C and commercially available carbon (E-Tek). Conditions: 0.5 M H_2SO_4 (O_2 purged), scan rate = 5 mV s^{-1}, rotation rate = 1600 rpm.

3.5. Fuel cell polarization experiments

During the fuel cell polarization tests, the current density was maintained constant for 3 min for each data point and the lowest cell potential value recorded during that period was reported. The polarization data obtained with a 5 cm^2 single cell are presented in Fig. 7. As expected, the performance is significantly improved when supplying pure oxygen on the cathode side instead of air. In the kinetic regime the voltage at current density of 2 mA cm^{-2} was increased from 0.85 V to 0.89 V as a result of the higher oxygen partial pressure. Furthermore, the peak power density increased from 0.23 W cm^{-2} to 0.34 W cm^{-2}. The onset of the mass transport limited regime, indicated by a slight increase of the slope of the *V–i* plot, occurred at ~0.7 A cm^{-2} with air and at ~1 A cm^{-2} with oxygen.

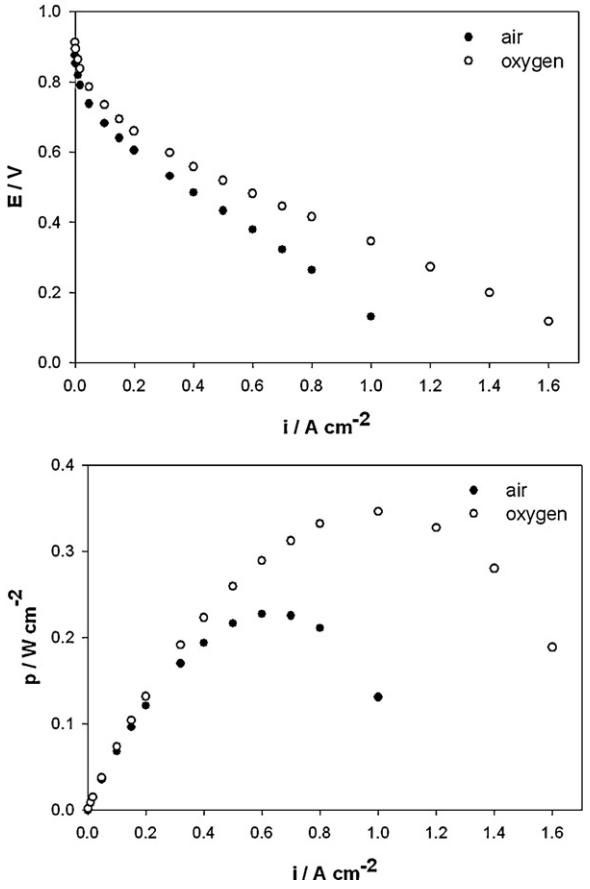

Fig. 7. Fuel cell polarization tests. Conditions: 100% relative humidity, 75 °C, oxidant flow rate = 1 l min^{-1}, hydrogen flow rate = 0.5 l min^{-1}, no backpressure applied.

4. Summary and conclusions

A ceramic–carbon composite based fuel cell catalyst support was synthesized by a process containing steps of electrospinning and heat treatment under reducing conditions. The support was coated with Pt nanoparticles using a microwave assisted polyol process to form a supported Pt catalyst. The electrochemical oxygen reduction performance and stability of this catalyst was assessed using cyclic voltammetry and rotating disk electrode techniques. The obtained oxygen reduction activity was comparable with that of a commercially available carbon supported Pt catalyst. Cyclic voltammetry tests showed a slight decrease in the active Pt area over 1000 cycles for the in-house prepared ceramic–carbon support catalyst. By contrast, the active Pt area loss was more pronounced for the commercial catalyst. Therefore the composite supported catalyst can be considered more stable compared to Pt/C. The support was found to be feasible for fuel cell operation, as was demonstrated by polarization tests using a single cell setup. However, the mass activity of the ceramic supported catalyst was still low, which is most likely due to the low conductivity and low surface area of ceramic support in this work, comparing to the carbon support reported in the literature. The high electrical conductivity of the Nb–TiO_2 relies on the heat treatment temperature at high temperatures. However, high temperature treatment leads to sintering and grain growth or agglomerations of ceramic particles. The effort to obtain high electrical conductivity with high surface areas is still needed for the ceramic support in the future.

Acknowledgments

The authors thank Lei Zhang and Ken Tsay for helpful discussions and assistance with conducting the fuel cell experiments. The financial support under the NRC-CNRS Cooperation Agreement “Nano-composite Catalysts for High Temperature PEM Fuel Cells” is gratefully acknowledged.

References

[1] K.-W. Park, K.-S. Seol, Electrochem. Commun. 9 (2007) 2256–2260.
[2] H. Chhina, D. Susac, S. Campbell, O. Kesler, Electrochem. Solid-State Lett. 12 (2009) B97–B100.
[3] X. Wang, W. Li, Z. Chen, M. Waje, Y. Yan, J. Power Sources 158 (2006) 154–159.
[4] E. Antolini, E.R. Gonzalez, Solid State Ionics 180 (2009) 746–763.
[5] N. Rajalakshmi, N. Lakshmi, K.S. Dhathathreyan, Int. J. Hydrogen Energy 33 (2008) 7521–7526.
[6] E. Forno, E. Lee, D. Campbell, Y. Xia, Nano Lett. 8 (2008) 668–672.
[7] H. Chhina, S. Campbell, O. Kesler, J. Electrochem. Soc. 156 (2009) B1232–B1237.
[8] W.-J. Lee, M. Alhosan, S.L. Yohe, N.L. Macy, W.H. Smyrl, J. Electrochem. Soc. 155 (2008) B915–B920.
[9] J. Bernard d'Arbigny, G. Taillades, M. Marrony, D.J. Jones, J. Rozière, Chem. Commun. 47 (2011) 7950–7952.
[10] S. Cavaliere, S. Subianto, J. Savych, D.J. Jones, J. Rozière, Energy Environ. Sci. 4 (2011) 4761–4785.
[11] A. Bauer, K. Lee, C. Song, Y. Xie, J. Zhang, R. Hui, J. Power Sources 195 (2010) 3105.
[12] X. Li, A.L. Zhu, W. Qu, H. Wang, R. Hui, L. Zhang, J. Zhang, Electrochim. Acta 55 (2010) 5891.
[13] N.V. Krstajic, et al., Surf. Sci. 601 (2007) 1949.
[14] T. Ioroi, Z. Siroma, N. Fujiwara, S.-I. Yamazaki, K. Yasuda, Electrochem. Commun. 7 (2005) 183.
[15] G. Chen, S.R. Bare, T.E. Mallouk, J. Electrochem. Soc. 149 (2002) A1092.
[16] S. Siracusano, V. Baglio, C. D'Urso, V. Antonucci, A.S. Aricò, Electrochim. Acta 54 (2009) 6292.

[17] S.-Y. Huang, P. Ganesan, S. Park, B.N. Popov, J. Am. Chem. Soc. Commun. 131 (2009) 13898.
[18] S.-Y. Huang, P. Ganesan, B.N. Popov, Appl. Catal. B 96 (2010) 224.
[19] S. von Kraemer, K. Wikander, G. Lindbergh, A. Lundblad, A.E.C. Palmqvist, J. Power Sources 180 (2008) 185–190.
[20] K. Wikander, H. Ekström, A.E.C. Palmqvist, A. Lundblad, K. Holmberg, G. Lindbergh, Fuel Cells 6 (2006) 21–25.
[21] L. Xiong, A. Manthiram, Electrochim. Acta 49 (2004) 4163–4170.
[22] J. Tian, G. Sun, M. Cai, Q. Mao, Q. Xin, J. Electrochem. Soc. 155 (2) (2008) B187–B193.
[23] A. Bauer, C. Song, A. Ignaszak, R. Hui, J. Zhang, L. Chevallier, D. Jones, J. Rozière, Electrochim. Acta 55 (2010) 8365.
[24] N. Rajalakshmi, N. Lakshmi, K.S. Dhathathreyan, Int. J. Hydrogen Energy 33 (2008) 7521.
[25] S. Shanmugam, A. Gedanken, J. Phys. Chem. C 113 (2009) 18707.
[26] V. Beachley, X. Wen, Mater. Sci. Eng. C 29 (2009) 663.
[27] W. Yu, W. Tu, H. Liu, Langmuir 15 (1999) 6.
[28] D.L. Boxall, G.A. Deluga, E.A. Kenik, W.D. King, C.M. Lukehart, Chem. Mater. 13 (2001) 891.
[29] X. Li, W.-X. Chen, J. Zhao, W. Xing, Z.-D. Xu, Carbon 43 (2005) 2168.
[30] F.C. Nart, W. Vielstich, Handbook of Fuel Cells: Fundamentals, Technology, and Applications, vol. 2, John Wiley and Sons Inc., Hoboken, NJ, 2003, p. 302.
[31] Z. Qi, P.G. Pickup, Chem. Commun. 21 (1998) 2299.